symmetry

Article

Particle Creation and Thermal Aspects of Viscous Generalized Cosmic Chaplygin Gas

Abdul Jawad *, Shamaila Rani and M. Adeel Sultan

Department of Mathematics, COMSATS University Islamabad, Lahore-Campus, Lahore-54000, Pakistan
* Correspondence: jawadab181@yahoo.com or abduljawad@cuilahore.edu.pk

Received: 19 June 2019; Accepted: 19 July 2019; Published: 12 August 2019

Abstract: We investigate the particle creation, as well as the thermodynamics phenomenon of viscous generalized cosmic Chaplygin gas as a cosmic fluid by assuming the flat FRW universe. For this purpose, we extract various parameters such as the energy density (ρ), Hubble parameter (H), declaration parameter (q), temperature (T_f), and particle number density (n) in the presence of three different models of the particle creation rate (Γ). We discuss the validity of the generalized second law of thermodynamics and thermal equilibrium condition under three models of Γ and discuss the graphical behavior of above-mentioned terms.

Keywords: particle creation; thermal aspects; viscous fluid; generalized cosmic Chaplygin gas

1. Introduction

Einstein gravity introduced the idea of a static universe by adding the cosmological constant in the field equation of general relativity. In 1922, Friedmann proposed the idea of an expanding universe. After that, researchers started research on the expanding universe. Furthermore, the evolution of the universe had been explained by non-equilibrium Muller [1], Israel and Stewart [2–4] (M-I-S) theory and Pavon et al. [5,6]. The difference in these ideas was finished when Hubble discovered novae in the Andromeda galaxy and demonstrated its distance to be way beyond the milky way's boundaries. The high-Z supernova research team and the supernova cosmology project were two different teams that were sent into space to collect data about astronomical objects [7,8]. The results were unpredicted, because the obtained results showed accelerated expansion of the universe [7,8].

Later on, the cosmic microwave background (CMB) [9] and Sloan Digital Sky Survey [10] also favored this accelerating phase of the universe. Through these observations, the researchers concluded that the cosmic acceleration was caused by exotic energy known as dark energy (DE) [11–14]. After this, much research has been done to discover the source, as well as properties of DE, but unfortunately, scientists failed to find a valid argument till now. The only known property of DE is the repulsive force. The simplest form of DE is the cosmological constant, but it faces two basic problems such as fine-tuning and cosmic coincidence. Alternative approaches such as modified theories of gravity and dynamical DE models have been assumed to illustrate the accelerated expansion scenario. The dynamical DE models include quintom [15–17], quintessence [18–20], the family of Chaplygin gas (CG) [21–23], K-essence [24–26], holographic DE models [27,28], etc. Moreover, the dark energy scenario has also been discussed through modified gravities such as Horndeski gravity [29], $f(R)$ gravity [30], mimetic gravity [31], $f(T)$ gravity [32], $f(G)$ gravity [33], and so on. A detailed discussion on DE models, as well as modified theories of gravity was also presented in [34].

Due to negative pressure of CG, it may be feasible for explaining DE. It is related to exotic fluid with negative pressure, but positive energy density. Various generalizations of CG have been suggested due to its effectivity for interpreting the expansion of the universe. The equation of state (EoS) of CG is modified by adding an ordinary matter agreeing with the current observational fallout CG named as modified CG [35]. The form that is generalized by adding any constant with an exponent over the energy density is termed as generalized CG (GCG) [36]. GCG with EoS $P = -\frac{B}{\rho^{\nu}}$ (where ν and B are positive constants) has been presented as an alternative model for depicting the cosmic acceleration. It is supposed to be a good verbal description of the accelerated expansion of the universe. In this spirit, the case $(1+\nu) > 0$ is thought provoking in the recent accelerated expansion in which GCG acts as dust for the primordial universe and DE with negative EoS for the present time universe. Another regime, $(1+\nu) < 0$, is also interesting [37] because GCG mimics initially the cosmological constant, but the EoS grows and behaves like dust with the passage of time. This behavior is good for the inflationary scenario as inflation occurs initially and then automatically ends at later times. Another modified form of the CG model is modified Chaplygin gas (MCG) [38]. There is a large amount of literature [39] investigating various aspects of the MCG to compare the standard cosmological model with recent observations.

Kamenshchik et al. [40] assumed that a spatially-flat FRW universe consists of CG and determined that the resulting evolution of the universe is consistent with the current observations of acceleration. The inflationary paradigm can be acquired by extrapolating the energy density in CG models [41]. The GCG put forward important alternations in the primordial universe. Moreover, Gonzalez-Diaz [42] proposed a generalized cosmic CG (GCCG) model such that the resulting models are physical, as well as stable even with the vacuum fluid satisfying the phantom condition. As MCG and GCG are more constrained as compared to GCCG, which can adapt itself to any domain of cosmology depending on the parameters, so the big-rip singularity can be easily avoided in this model.

The generalized cosmic Chaplygin gas (GCCG) is the extended form of CG, and its equation of state is given by [42]:

$$p = -\rho^{-\lambda}\left(A + (\rho^{1+\lambda} - A)^{-\omega}\right), \tag{1}$$

where p is the pressure, ρ is the energy density, $A = \frac{D}{1+\omega} - 1$, and the value of D may be positive or negative. The value of λ is taken as positive, and the value of ω must be taken in the range of $-l < \omega < 0$, where l is greater then one, i.e $l > 1$. This EoS reduces to that of current Chaplygin unified models for dark matter and dark energy in the limit $\omega \to 0$ and satisfies the conditions: (i) it becomes a de Sitter fluid at late time and when $\omega = -1$; (ii) it reduces to $p = \rho$ in the limit that the Chaplygin parameter $D \to 0$; (iii) it also reduces to the EOS of current Chaplygin unified dark matter models at high energy density; and (iv) the evolution of density perturbations derived from the chosen EoS becomes free from the pathological behavior of the matter power spectrum for physically-reasonable values of the involved parameters at late time. This EoS shows the dust era in the past and ΛCDM in the future.

Black hole (BH) physics introduced the idea of thermodynamics in cosmology. Hawking [43] proposed that the temperature (T) produced by BHs and the surface gravity of the event horizon are proportional to each other. The correspondence of the Einstein field equations, as well as thermodynamics was proposed by Jacobson [44]. He determined this connection based on entropy-horizon area proportionality with the Clausius relation i.e., $dQ = TdS$ (which is also known as first law of thermodynamics), where T, dS, and dQ demonstrate the temperature, change in entropy, as well as change in energy, respectively. For any horizon, field equations of spherically-symmetric space time can be shown as $TdS = dE + PdV$, where V expresses the volume, P denotes pressure, and E represents the internal energy for the spherical system [45].

The generalized Second Law of Thermodynamics (GSLT) is the most considerable topic to examine the expanding behavior of the universe. The GSLT can be defined as the sum of all the entropies, i.e., inside the horizon, and the entropy of boundaries always increases with time [46]. A plethora of work has been done by various people in order to investigate the validity of GSLT by assuming the usual entropy [47], power law corrected entropy [48], and logarithmic corrected entropy [49]. Furthermore, some people have examined the validity of GSLT under different systems including the interaction of two [50], as well as three components of fluid [51] in the Friedmann–Robertson–Walker (FRW) universe by taking the simple horizon entropy of the universe.

The matter creation in an expanding universe is not a new issue in cosmology. Such a physical mechanism has been intensively investigated. Zeldovich [52] described the process of the creation of matter in the cosmological context through an effective mechanism. Prigogine [53] studied how to insert the creation of matter consistently in Einstein's field equations. Many authors have explored scenarios of matter creation in cosmology, but here, we are particularly interested in the gravitationally-induced particle creation scenario denominated the creation of cold dark matter (CCDM) [54]. The relativistic second order thermodynamic theories of Muller [1], Israel and Stewart [2–4], and Pavon et al. [5,6] play a crucial role in describing the evolution of the Universe as a sequence of dissipative processes. The theory proposes that deviations from equilibrium described by bulk stress, heat flow, and shear stress can be treated as independent dynamical variables bounded by average molecular speed, thereby ensuring causality. The particle creation mechanism driving bulk viscous pressure has been extensively used to describe the dynamics and evolution of the early universe including early inflation and current accelerated expansion [55]. Particle creation has also been related to an emergent universe [56]. Moreover, Brevik [57] did a versatile study on viscous fluid by assuming homogeneous, as well as inhomogeneous EoS. Viscous cosmology in the early universe was investigated, examining the viscosity effects on the various inflationary observables. Additionally, viscous cosmology in the late universe was studied, containing current acceleration and the possible future singularities, and we investigate how one may even unify inflationary and late-time acceleration. The viscosity-induced crossing through the quintessence-phantom divide was also analyzed, and we examine the realization of viscosity-driven cosmological bounces and also briefly mention how the Cardy–Verlinde formula is affected by viscosity.

Bhattacharya et al. [58] studied the cosmic scenario and thermodynamics in the presence of MCG and adiabatic matter creation. Jawad et al. [59] discussed the thermodynamics of the gravitationally-induced particle creation scenario in the DGPbraneworld. In the present paper, we investigate the particle creation, as well as the thermodynamics phenomenon in the presence of the viscous-inspired GCCG model. In this way, we develop various basic parameters in Section 2. In Section 3, we discuss the entropy production phenomenon. We discuss GSLT and the thermal equilibrium condition in Section 4. We summarize our results in the last section.

2. Particle Creation and GCCG

The energy momentum tensor $T^{\mu\nu}$ regarding the bulk viscosity of relativistic fluid is defined as:

$$T^{\mu\nu} = (\rho + p + \Pi)u^{\mu}u^{\nu} + (p + \Pi)g^{\mu\nu}, \tag{2}$$

and here the terms ρ, p, Π, and u^{μ} are known as energy density, thermodynamics pressure, bulk viscous pressure, and four-velocity respectively. The entropy flow vector under the scenario of second order non-equilibrium thermodynamics is defined as: [3]

$$S^{\mu} = sN^{\mu} - \frac{\tau\Pi^2}{2\zeta T_f}u^{\mu}, \tag{3}$$

where the terms s, N^{μ}, τ, ζ, and T_f are named as the entropy per particle, the particle flow vector, relaxation time, the coefficient of bulk viscosity, and the temperature of cosmic fluid, respectively. In the above equation, $N^{\mu} = nu^{\mu}$, where n is the particle number density. Now, Γ is defined as:

$$\Gamma = \frac{\dot{N}}{N}, \tag{4}$$

where $N = na^3$ is the number of particles in a co-moving volume (a^3). $\Gamma < 0$ and $\Gamma > 0$ mean particle annihilation and production, respectively. The entropy production density is created due to the change in the particle number density and mathematically can be expressed as:

$$S^{\mu}_{;\mu} = -\frac{\Pi}{T_f}\left(3H + \frac{\tau}{s}\dot{\Pi} + \frac{1}{2}\Pi T_f(\frac{\tau}{\zeta T_f}u^{\mu})_{;\mu} + \varepsilon\frac{n\Gamma}{\Pi}\right), \tag{5}$$

ε gives the chemical potential. The second law of thermodynamics is valid if we take $S^{\mu}_{;\mu} = \frac{\Pi^2}{\zeta T_f} \geq 0$. The non-linear differential equation of bulk viscosity (Π) can be obtained by taking $S^{\mu}_{;\mu} = \frac{\Pi^2}{\zeta T_f} \geq 0$ and has the following relation [60]:

$$\Pi^2\left(1 + \frac{1}{2}T_f(\frac{\tau}{\zeta T_f}u^{\mu})_{;\mu} + \tau\Pi\dot{\Pi} + 3H\zeta\Pi\right) = -\zeta\varepsilon n\Gamma. \tag{6}$$

Consequently, any change from equilibrium described by Π and the single causal theory is affirmed with the help of Γ. Furthermore, the conservation equations in the presence of Γ are given as:

$$N^{\mu}_{;\mu} = n\Gamma \quad \text{and} \quad T^{\mu\nu}_{;\nu} = 0, \tag{7}$$

which leads to:

$$\dot{n} + 3Hn = n\Gamma, \tag{8}$$

and:

$$\dot{\rho} + 3H(\rho + p + \Pi) = 0, \tag{9}$$

where $\dot{n} = u_{,\mu}n^{\mu}$. Thus, the Gibbs relation has the following form:

$$T_f ds = d(\frac{\rho}{n}) + pd(\frac{1}{n}). \tag{10}$$

By comparing the Gibbs relation with Equations (8) and (9), we get:

$$nT_f\dot{s} = -3H\Pi - (\rho + p)\Gamma. \tag{11}$$

We assume p and ρ as a function of the thermodynamic variables n and T_f. By utilizing Equations (8) and (9), we have:

$$\frac{\partial\rho}{\partial n} = \frac{p+\rho}{n} - \frac{T_f}{n}\frac{dp}{dT_f}, \tag{12}$$

and the temperature of the cosmic fluid is:

$$\frac{\dot{T}_f}{T_f} = -3H\left(\frac{\frac{\partial p}{\partial T_f}}{\frac{\partial\rho}{\partial T_f}} + \frac{\Pi}{T_f\frac{\partial\rho}{\partial T_f}}\right) + \Gamma\left(\frac{\frac{\partial\rho}{\partial T_f}}{\frac{\partial p}{\partial T_f}} - \frac{\rho+p}{\frac{\partial\rho}{\partial T_f}}\right). \tag{13}$$

By using Equation (11) with the last equation, we obtain the following expression:

$$\frac{\dot{T}_f}{T_f} = -(3H - \Gamma)\frac{\frac{\partial p}{\partial T_f}}{\frac{\partial\rho}{\partial T_f}} + \frac{n\dot{s}}{\frac{\partial\rho}{\partial T_f}}. \tag{14}$$

We observe that the temperature and viscous pressure (Π) are effected by particle production. We find a relation of viscous pressure as a function of particle production rate by taking $\dot{s} = 0$, in the following form:

$$\Pi = -\frac{\Gamma}{3H}(\rho + p). \tag{15}$$

The change in particle number density (n) explains cosmic fluid, and the change in the temperature of cosmic fluid is:

$$\frac{\dot{T}_f}{T_f} = -(3H - \Gamma)\frac{\partial p}{\partial \rho}, \tag{16}$$

so n can be obtained from Equation (8) for isentropic particle production as:

$$\frac{\dot{n}}{n} = -(3H - \Gamma). \tag{17}$$

The Friedmann equation for FRW cosmology is given as:

$$H^2 = \frac{\kappa\rho}{3} = \frac{\rho}{3}. \tag{18}$$

where $\kappa = 8\,\pi G$. By using Equation (9), the derivative of H turns out to be:

$$\dot{H} = -\frac{\kappa(\rho + p + \Pi)}{2} = -\frac{(\rho + p + \Pi)}{2}. \tag{19}$$

We can take GCCG as the cosmic fluid, then find the expression for energy density ρ with the combination of Equations (1) and (9) as:

$$\rho = \left(A + \left(1 + ca^{-3\mu}e^{\mu\int\Gamma dt}\right)^{\frac{1}{1+\omega}}\right)^{\frac{1}{1+\lambda}}, \tag{20}$$

where $\mu = (1 + \lambda)(1 + \omega)$ and c are constants. In this way, the Hubble parameter can be expressed as:

$$H = \frac{1}{\sqrt{3}}\left(A + \left(1 + ca^{-3\mu}e^{\mu\int\Gamma dt}\right)^{\frac{1}{1+\omega}}\right)^{\frac{1}{2+2\lambda}}. \tag{21}$$

By using Equations (15), (19), and (21), the deceleration parameter $q = -1 + \frac{\dot{H}}{H^2}$ has the following form:

$$q = -1 + \frac{3}{2}\left(1 - \frac{\Gamma}{3H}\right)\left(\frac{1 - (1 + ca^{-3\mu}e^{\mu\int\Gamma dt})^{-\omega}}{1 + A(1 + ca^{-3\mu}e^{\mu\int\Gamma dt})^{\frac{-1}{1+\omega}}}\right). \tag{22}$$

With the help of Equations (16) and (17), T_f and n can be expressed as:

$$T_f = \frac{T_c\rho^{-\lambda}c^{\frac{\mu-1}{\mu}}a^{-3(\mu-1)}e^{(\mu-1)\int\Gamma dt}}{(1 + ca^{-3\mu}e^{\mu\int\Gamma dt})^{\frac{\omega}{1+\omega}}}, \tag{23}$$

$$n = n_c c^{\frac{1}{\mu}}a^{-3}e^{\int\Gamma dt}, \tag{24}$$

and here, T_c and n_c are the constants of integration. It is shown that the parameters of thermodynamics, as well as dynamics, which are given in Equations (20)–(24), are changed with respect to particle creation rate Γ. Hence, the cosmic evolution of the universe can be studied by particular selection of Γ.

Recently, accelerating cosmology driven by the gravitationally-induced adiabatic (entropy per particle remains constant during the process) particle production has intensively been examined in the FLRW universe [54,61–70]. Further, it has also been discussed that not only the current accelerating universe, but the particle production can also be taken into account for the early inflationary universe [70]. In fact, it has been shown that the matter creation models can provide an alternative cosmology known as the CCDM (creation cold dark matter) cosmology [54,60,64], which is a viable alternative to the ΛCDM model, both at background and perturbative levels [66]. Additionally, the effects of adiabatic particle production have been tested at the cosmic microwave background level [67], which shows a close behavior to that of ΛCDM. In fact, it has been argued that adiabatic particle production can provide a possible connection between the early and late accelerating regimes [68]. Further, it has been argued that a complete cosmic scenario with early and late de Sitter eras can also be encountered by such a mechanism [65]. The stability of such models in agreement with the generalized second law of thermodynamics has been studied [61,71]. However, the key point in all such models driven by the gravitational particle production is to consider several choices for the rate of particle production, which in general are considered to be the functions of the Hubble rate of the FLRW universe.

Here, we choose three different models of Γ as:

- Model 1: $\Gamma = 15\beta H\Big(1 - a\tanh(10 - 12a)\Big)$
- Model 2: $\Gamma = 15\beta H\Big(1 - a^{1+m}\Big)$
- Model 3: $\Gamma = 15\beta H\dfrac{\left(H^{2\lambda+2} - \frac{A}{3^{\lambda+1}}\right)^{\omega+1} - \frac{1}{3^{\mu}}}{\left(H_0^{2\lambda+2} - \frac{A}{3^{\lambda+1}}\right)^{\omega+1} - \frac{1}{3^{\mu}}}.$

The first two models depend on the scale factor and the third model on the Hubble parameter. Here, m belongs to real numbers, but $m \neq -1$, β is any positive constant. Recently, the phantom behavior of particle creation has been examined in a similar form to Model 1 [63]. It has been discovered that Γ is proportional to ρ, when the universe is dominated by bulk viscosity for perfect fluid [72]. Hence, we can say that there is some relation between Γ and ρ, when the universe is dominated by bulk viscosity for exotic fluid (like GCCG). Therefore, we select Γ in the term of H in Model 3.

2.1. Model 1: $\Gamma = 15\beta H\Big(1 - a\tanh(10 - 12a)\Big)$

Here, we assume $\theta = 10 - 12a$, and by substituting this value of Γ in Equations (20)–(24), we have:

$$-\rho = \left(A + \left(1 + ca^{(15\beta-3)\mu}\cosh^{\frac{5\beta\mu}{4}}\theta\right)^{\frac{1}{1+\omega}}\right)^{\frac{1}{1+\lambda}}, \tag{25}$$

$$H = \frac{1}{\sqrt{3}}\left(A + \left(1 + ca^{(15\beta-3)\mu}\cosh^{\frac{5\beta\mu}{4}}\theta\right)^{\frac{1}{1+\omega}}\right)^{\frac{1}{2+2\lambda}}, \tag{26}$$

$$\begin{aligned} q &= -1 - \frac{3}{2}\Big(1 - 5\beta(1 - a\tanh\theta)\Big)\left(\left(1 + c\cosh^{\frac{5\beta\mu}{4}}\theta a^{3\mu(5\beta-1)}\right)^{-\omega}\right. \\ &- \left.1\right)\left(1 + A(1 + ca^{3\mu(5\beta-1)}\cosh^{\frac{5\beta\mu}{4}}\theta)^{\frac{-1}{1+\omega}}\right)^{-1}. \end{aligned} \tag{27}$$

$$T_f = \frac{T_c\rho^{-\lambda}c^{\frac{\mu-1}{\mu}}a^{(\mu-1)(15\beta-3)}\cosh^{\frac{5\beta\mu}{4}}\theta}{(1 + ca^{3(5\beta-1)\mu}\cosh^{\frac{5\beta\mu}{4}}\theta)^{\frac{\omega}{1+\omega}}}. \tag{28}$$

$$n = n_c c^{\frac{1}{\mu}}a^{15\beta-3}\cosh^{\frac{5\beta\mu}{4}}\theta. \tag{29}$$

In Figure 1, q shows the negative behavior versus a, which represents the accelerated phase of the universe. The ranges of this parameter lie within the constraints as mentioned in [73]. Figure 2 exhibits the positive behavior of T_f versus a, which shows that the temperature of the system is increasing. Figure 3 shows the positive behavior of n corresponding to a, which means particles are being produced.

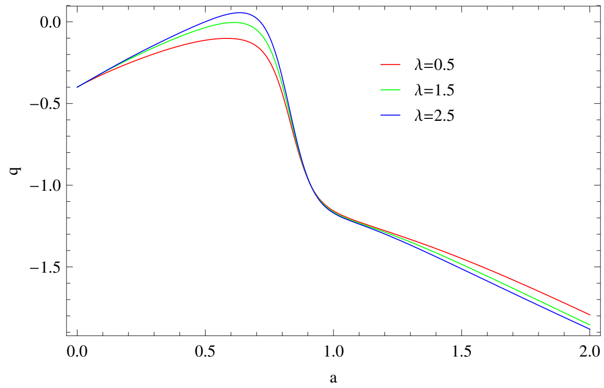

Figure 1. q versus a for Model 1 with $A = \frac{1}{3}$, $\beta = 0.12$, $c = 5$, and $\omega = 0.5$.

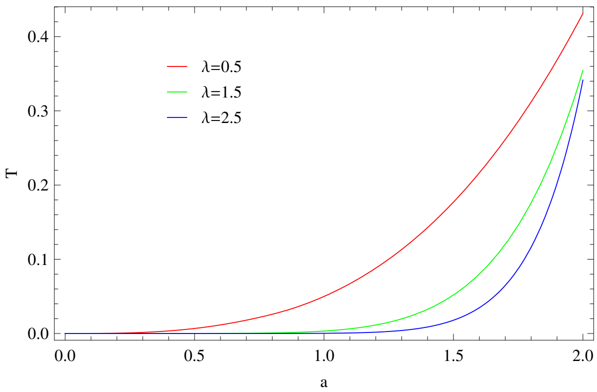

Figure 2. $T(\ K)$ versus a for Model 1.

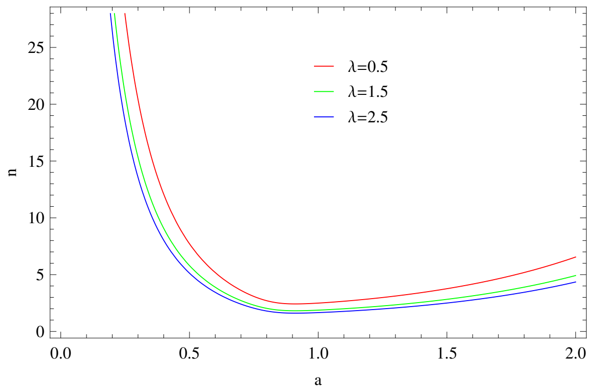

Figure 3. n versus a for Model 1.

2.2. *Model 2:* $\Gamma = 15\beta H\left(1 - a^{1+m}\right)$

For this model, Equations (20)–(24) can be written as:

$$\rho = \left(A + \left(1 + ca^{3\mu(\beta-1)}e^{\frac{3\beta\mu a^{m+1}}{m+1}}\right)^{\frac{1}{1+\omega}}\right)^{\frac{1}{1+\lambda}}, \tag{30}$$

$$H = \frac{1}{\sqrt{3}}\left(A + \left(1 + ca^{3\mu(\beta-1)}e^{\frac{3\beta\mu a^{m+1}}{m+1}}\right)^{\frac{1}{1+\omega}}\right)^{\frac{1}{2+2\lambda}}, \tag{31}$$

$$\begin{aligned} q &= -1 - \frac{3}{2}\left(1 - \beta(1 + a^{1+m})\right)\left(\left(1 + ca^{3\mu(\beta-1)}e^{\frac{3\beta\mu a^{m+1}}{m+1}}\right)^{-\omega} \right. \\ &- \left. 1\right)\left(1 + A\left(1 + ca^{3\mu(\beta-1)}e^{\frac{3\beta\mu a^{m+1}}{m+1}}\right)^{\frac{-1}{1+\omega}}\right)^{-1}. \end{aligned} \tag{32}$$

$$T_f = \frac{T_c\rho^{-\lambda}c^{\frac{\mu-1}{\mu}}a^{3(\beta-1)(\mu-1)}e^{\frac{3\beta(\mu-1)a^{m+1}}{m+1}}}{(1 + ca^{-3\mu}e^{\frac{3\beta\mu a^{m+1}}{m+1}})^{\frac{\omega}{1+\omega}}}. \tag{33}$$

$$n = n_c c^{\frac{1}{\mu}}a^{3(\beta-1)}e^{\frac{3\beta\mu a^{m+1}}{m+1}}. \tag{34}$$

Figure 4 shows the positive, as well as negative behavior of q in different ranges of a. For $\alpha = 0.5$, q shows the deceleration phase of the universe in the range of $a < 0.75$ and the accelerated phase of the universe in the range of $a \geq 0.75$. For $\alpha = 1.5$ and $\alpha = 2.5$, q shows the deceleration phase of the universe in the range of $a < 0.9$ and the accelerated phase of the universe in the range of $a \geq 0.9$. The ranges of this parameter lie within the constraints as mentioned in [73]. Figure 5 exhibits the positive behavior of T_f versus a, which shows that the temperature of the system is decreasing. Figure 6 shows the positive behavior of n corresponding to a, which mean particles are being produced.

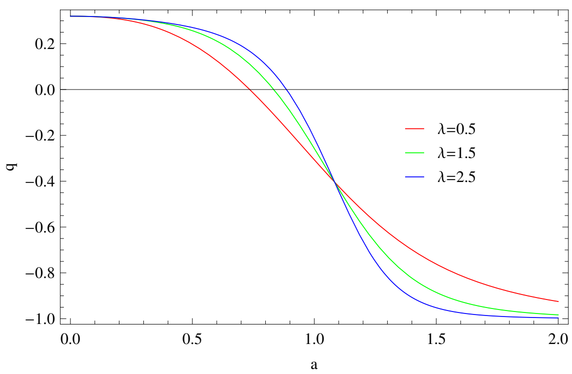

Figure 4. q versus a for Model 2 by taking $m = 1$.

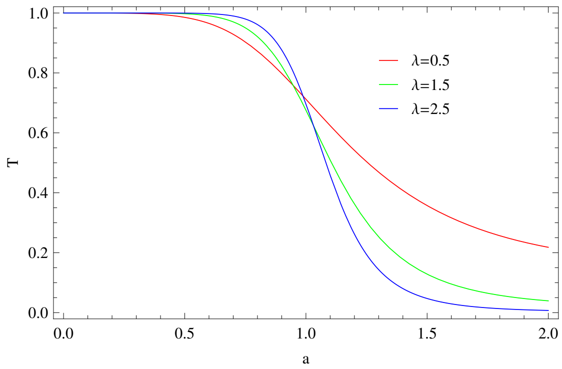

Figure 5. $T(\,K)$ versus a for Model 2.

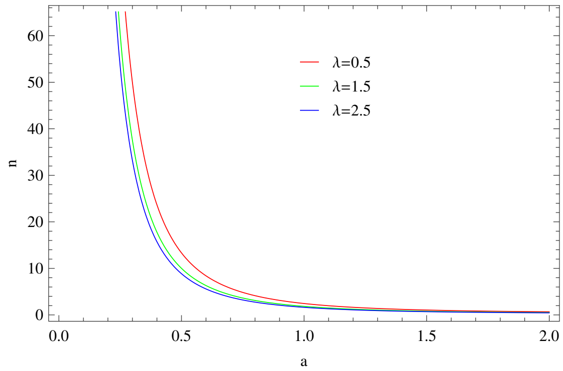

Figure 6. n versus a for Model 2.

2.3. Model 3: $\Gamma = 15\beta H \dfrac{\left(H^{2\lambda+2}-\frac{A}{3\lambda+1}\right)^{\omega+1}-\frac{1}{3^{\mu}}}{\left(H_0^{2\lambda+2}-\frac{A}{3\lambda+1}\right)^{\omega+1}-\frac{1}{3^{\mu}}}$

By using the above expression of Γ, Equations (20)–(24) turn out to be:

$$\rho = \left(A+\left(\frac{(\rho_0^{1+\lambda}-A)^{1+\omega}}{r}+1-\frac{1}{r}\right)^{\frac{1}{1+\omega}}\right)^{\frac{1}{1+\lambda}}, \tag{35}$$

$$H = \left(\frac{A}{3^{1+\lambda}}+\left(\frac{y_0}{r}+\frac{1}{3^{\mu}}\right)^{\frac{1}{1+\omega}}\right)^{\frac{1}{2+2\lambda}}, \tag{36}$$

$$q = -1+\frac{3}{2}\frac{3^{\frac{\omega\lambda}{1+\lambda}}(r-\beta)y_0}{\left(y_0-\frac{r}{3^{\mu}}\right)^{\frac{\omega}{1+\omega}}\left(\frac{A}{3^{1+\lambda}}+\left(y_0-\frac{r}{3^{\mu}}\right)^{\frac{1}{1+\omega}}\right)}. \tag{37}$$

$$T_f = T_0\rho^{-\lambda}(\rho^{1+\lambda}-A)^{-\omega}\left(\frac{1}{r}\right)^{\frac{\mu-1}{\mu}}. \tag{38}$$

$$n = \frac{n_0}{r^{\frac{1}{\mu}}}. \tag{39}$$

Here, $y_0 = \left(H_0^{2\lambda+2}-\frac{A}{3\lambda+1}\right)^{\omega+1}-\frac{1}{3^{\mu}}$, $r = \beta+(1-\beta)\left(\frac{a}{a_0}\right)^{3\mu}$, and $H = H_0$ for $a = a_0$. In Figure 7, q shows the positive behavior versus a, which represents the decelerated phase of the universe. Figure 8 exhibits the positive behavior of T_f versus a, which shows that the temperature of the system is decreasing. Figure 9 exhibits the positive behavior of n versus a, which means particles are being produced.

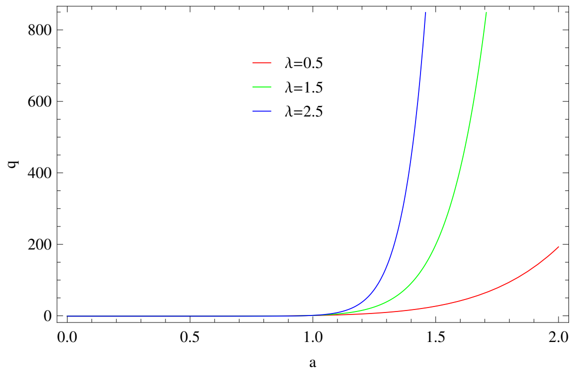

Figure 7. q versus a for Model 3 by taking $a_0 = 1$, $H_0 = 67$, and the same constants.

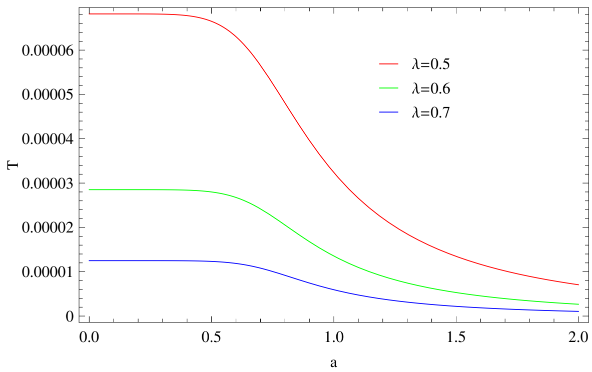

Figure 8. $T(\ K)$ versus a for Model 3.

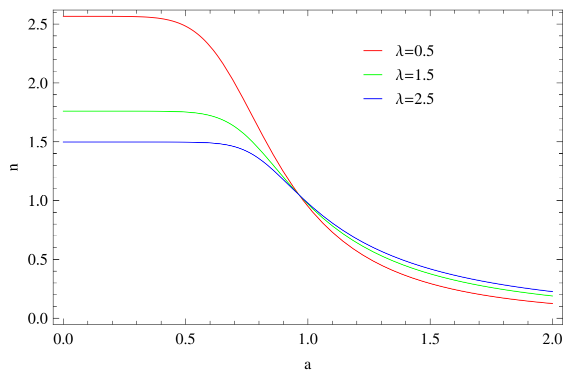

Figure 9. n versus a for Model 3.

3. Entropy Production

The change in entropy per particle can be obtained by substituting Equations (8) and (9) in (11) as:

$$nT_f\dot{s} = \dot{\rho} - \frac{\dot{n}}{n}(\rho + P), \tag{40}$$

which leads to:

$$\frac{nT_f X\dot{s}\rho^{\lambda}}{\rho^{1+\lambda} - A} = \frac{1}{1+\lambda}\frac{dX}{dt} + n^{-(1+\lambda)}\frac{dY}{dt}, \tag{41}$$

where:

$$X=\frac{(\rho^{1+\lambda}-A)^{1+\omega}}{n^{1+\lambda}},\quad Y=\log n-\frac{\omega(\rho^{1+\lambda}-A)^{1+\omega}}{\mu}. \tag{42}$$

By substituting Equation (8) and $\Pi=-\rho(\gamma+\frac{2\dot{H}}{3H^2})$ in Equation (13), we get the temperature of the fluid as:

$$T_f=T_i e^{\int_{n_i}^{n}\frac{v-\gamma u}{n}dn+\int_{\rho_i}^{\rho}u\frac{d\rho}{\rho}}. \tag{43}$$

In this way, Equation (41) can be written as:

$$\frac{n\rho^{\lambda}\dot{s}T_i}{(\rho^{1+\lambda}-A)}e^{(\int_{n_i}^{n}\frac{v-ru}{n}dn+\int_{\rho_i}^{\rho}u\frac{d\rho}{\rho})}=\frac{1}{1+\lambda}\frac{dX}{dt}+n^{-(1+\lambda)}\frac{dY}{dt}, \tag{44}$$

and here, i stands for the initial time, $\gamma=\frac{p+\rho}{\rho}$, $u=\frac{\rho}{T_f\partial\rho/\partial T_f}$, and $v=\frac{\partial p/\partial T_f}{\partial\rho/\partial T_f}$. In the inflationary phase, we consider $\rho=\rho_i$ and $H=H_i$. Thus, Equation (44) turns out to be:

$$\dot{s}=\alpha_i n^{\gamma_i u_i-v_i-1}(3H_i-\Gamma), \tag{45}$$

where $\alpha_i=\frac{\rho_i\gamma_i}{T_i n_i^{\gamma_i u_i-v_i}}$. For $\gamma_i=\frac{4}{3}$, $u_i=1$, and $v_i=\frac{1}{3}$, we get $\alpha_i=\frac{4\rho_i}{3T_i n_i}$, and the above equation becomes:

$$\dot{s}=\alpha_i(3H_i-\Gamma), \tag{46}$$

which leads to:

$$s=\alpha_i\left(3(t-t_i)H_i-\int_{t_i}^{t}\Gamma\right)+s_i. \tag{47}$$

The above equation shows that s also depends on Γ. Thus, the relation of the change in entropy for a co-moving volume can be written as $\varepsilon=sna^3=sN$ by taking GCCG as matter, and similar results were obtained in [60]. Hence, we can write ε by using the above results as:

$$\varepsilon=\left(\alpha_i\left(3(t-t_i)H_i-\int_{t_i}^{t}\Gamma\right)+s_i\right)N_i e^{\int_{t_i}^{t}\Gamma dt}. \tag{48}$$

The de Sitter phase of GCCG has an exponential increase in co-moving entropy and $\Gamma\neq 0$ represented by Equation (48). Then, it was observed that GCCG as a cosmic fluid exhibits similar results concluded for normal fluid in [60].

4. Thermodynamical Analysis

The Hubble parameter and apparent horizon (R_A) coincide with each other for a flat FRW universe such as $R_A=\frac{1}{H}$. Thus, the derivative of R_A w.r.t time t is given as:

$$\dot{R_A}=-\frac{\dot{H}}{H^2}=-\frac{1}{2}\left(1-\frac{\Gamma}{3H}\right)\left(\frac{(3^{1+\lambda}H^{2+2\lambda}-A)^{\omega+1}-1}{3^{\lambda-1}H^{2+2\lambda}(3^{1+\lambda}H^{2+2\lambda}-A)^{\omega}}\right). \tag{49}$$

Bekenstein entropy [46] is given as:

$$S_A=\left(\frac{c^3}{G\hbar}\right)\frac{4\pi R_A^2}{4}=\frac{1}{8}R_A^2, \tag{50}$$

and the Hawking temperature [43] of the horizon is:

$$T_A=\left(\frac{c\hbar}{\kappa_B}\right)\frac{1}{2\pi R_A}=\frac{4}{R_A}. \tag{51}$$

The first law of thermodynamics [44] has the following form:

$$-dE_A = T_A dS_A, \tag{52}$$

and here, dE_A represents the amount of energy for the apparent horizon [74], having the following relation:

$$dE_A = \frac{R_A^3}{2}(\rho + p + \Pi)Hdt = \frac{R_A^3}{2}(\rho + p)\left(1 - \frac{\Gamma}{3H}\right)Hdt. \tag{53}$$

By substituting the values dE_A and T_A, Equation (52) turns out to be:

$$\begin{aligned} \dot{S_A} = & -\frac{3^{\frac{3}{2}}}{8}\left(1 - \frac{\Gamma}{3H}\right)\left(A + \left(1 + ca^{-3\mu}e^{\mu\int \Gamma dt}\right)^{\frac{1}{1+\omega}}\right)^{\frac{-1}{2+2\lambda}} \\ & \times \frac{1 - \left(1 + ca^{-3\mu}e^{\mu\int \Gamma dt}\right)^{\frac{1}{1+\omega}}}{1 + A\left(1 + ca^{-3\mu}e^{\mu\int \Gamma dt}\right)^{\frac{-1}{1+\omega}}}, \end{aligned} \tag{54}$$

where H can be taken from Equation (21).

However, GSLT is defined as $\dot{S}_T = \dot{S}_A + \dot{S}_f \geq 0$, which means the total entropy of the system never decreases. Thus, the Gibbs relation can be written as:

$$T_f dS_f = dE_f + pdV, \tag{55}$$

where $E_f = \rho V$ and S_f are known as the energy and entropy of cosmic fluid, respectively. Thus, the derivative of S_f is given as:

$$\begin{aligned} \dot{S_f} = & \left(1 - \frac{\Gamma}{3H}\right)\frac{-9c^{\frac{1}{\mu}}a^{-3}e^{\int \Gamma dt}(4T_c)^{-1}}{(A + (1 + ca^{-3\mu}e^{\mu\int \Gamma dt})^{\frac{1}{1+\omega}})^{\frac{1}{1+\lambda}}} \\ & \times\left(\frac{1 - (1 + ca^{-3\mu}e^{\mu\int \Gamma dt})^{-\omega}}{1 + A(1 + ca^{-3\mu}e^{\mu\int \Gamma dt})^{\frac{-1}{1+\omega}}} + 2\right). \end{aligned} \tag{56}$$

Hence, $\dot{S_T}$ can be obtained by adding Equations (56) and (58):

$$\begin{aligned} \dot{S_T} = & -\frac{3^{\frac{3}{2}}}{8}\left(1 - \frac{\Gamma}{3H}\right)\left(A + (1 + ca^{-3\mu}e^{\mu\int \Gamma dt})^{\frac{1}{1+\omega}}\right)^{\frac{-1}{2+2\lambda}} \\ & \times\left(\frac{1 - (1 + ca^{-3\mu}e^{\mu\int \Gamma dt})^{-\omega}}{1 + A(1 + ca^{-3\mu}e^{\mu\int \Gamma dt})^{\frac{-1}{1+\omega}}} + \frac{2\sqrt{3}c^{\frac{1}{\mu}}a^{-3}e^{\int \Gamma dt}}{T_c}\right. \\ & \times(A + (1 + ca^{-3\mu}e^{\mu\int \Gamma dt})^{\frac{1}{1+\omega}})^{\frac{-1}{1+\lambda}}\left((1 - (1 + ca^{-3\mu}\right. \\ & \left.\left.\times e^{\mu\int \Gamma dt})^{\frac{1}{1+\omega}})\frac{1}{1 + A(1 + ca^{-3\mu}e^{\mu\int \Gamma dt})^{\frac{-1}{1+\omega}}} + 2\right)\right). \end{aligned} \tag{57}$$

Model 1: $\Gamma = 15\beta H\Big(1 - a\tanh\theta\Big)$

For $\theta = 10 - 12a$ and substituting this value of Γ in Equation (57), we have:

$$\begin{aligned}\dot{S_T} &= \frac{-3^{\frac{3}{2}}}{8}(1-5\beta(1-a\tanh\theta))(A+(1+ca^{-3\mu+15\beta}\cosh^{\frac{5\beta\mu}{4}}\theta \\ &)^{\frac{1}{1+\omega}})^{\frac{-1}{2+2\lambda}}\Bigg(\frac{1-(1+ca^{-3\mu+15\beta}\cosh^{\frac{5\beta\mu}{4}}\theta)^{\frac{1}{1+\omega}}}{1+A(1+ca^{-3\mu+15\beta}\cosh^{\frac{5\beta\mu}{4}}\theta)^{\frac{-1}{1+\omega}}}+\frac{2\sqrt{3}c^{\frac{1}{\mu}}}{T_c} \\ &\times a^{-3+15\beta}\cosh^{\frac{5\beta\mu}{4}}\theta(A+(1+ca^{-3\mu+15\beta}\cosh^{\frac{5\beta\mu}{4}}\theta)^{\frac{1}{1+\omega}})^{\frac{-1}{1+\lambda}} \\ &\times\Bigg(\frac{(1-(1+ca^{3\mu(5\beta-1)}\cosh^{\frac{5\beta\mu}{4}}\theta)^{\frac{1}{1+\omega}})}{1+A(1+ca^{-3\mu(1-5\beta)}\cosh^{\frac{5\beta\mu}{4}}\theta)^{\frac{-1}{1+\omega}}}+2\Bigg)\Bigg).\end{aligned} \tag{58}$$

The plot of $\dot{S_T}$ versus a for three different values of λ is shown in Figure 10 for Model 1, which shows the validity of GSLT in the range of $0.91 \leq a \leq 2$ and does not exhibit validity in the range of $0 < a < 0.90$, for the same constants.

Model 2: $\Gamma = 3\beta H\Big(1 + a^{1+m}\Big)$

By substituting this model in Equation (57), we get:

$$\begin{aligned}\dot{S_T} &= -\frac{3^{\frac{3}{2}}}{8}(1-\beta(1+a^{1+m}))(A+(1+ca^{3\mu(\beta-1)}e^{\beta\mu\frac{a^{m+1}}{m+1}} \\ &)^{\frac{1}{1+\omega}})^{\frac{-1}{2+2\lambda}}\Bigg(\frac{1-(1+ca^{3\mu(\beta-1)}e^{\beta\mu\frac{a^{m+1}}{m+1}})^{\frac{1}{1+\omega}}}{1+A(1+ca^{3\mu(\beta-1)}e^{\beta\mu\frac{a^{m+1}}{m+1}})^{\frac{-1}{1+\omega}}}+\frac{2\sqrt{3}}{T_c} \\ &\times c^{\frac{1}{\mu}}a^{3(\beta-1)}e^{\beta\mu\frac{a^{m+1}}{m+1}}(A+(1+ca^{3\mu(\beta-1)}e^{\beta\mu\frac{a^{m+1}}{m+1}})^{\frac{1}{1+\omega}})^{\frac{-1}{1+\lambda}} \\ &\times\Bigg(\frac{1-(1+ca^{3\mu(\beta-1)}e^{\beta\mu\frac{a^{m+1}}{m+1}})^{\frac{1}{1+\omega}}}{1+A(1+ca^{3\mu(\beta-1)}e^{\beta\mu\frac{a^{m+1}}{m+1}})^{\frac{-1}{1+\omega}}}+2\Bigg)\Bigg).\end{aligned} \tag{59}$$

The plot of $\dot{S_T}$ versus a for three different values of λ is shown in Figure 11 for Model 2. The graph does not show the validity in the range $0 < a < 1.4$ and shows the validity of GSLT in the range of $1.4 \leq a \leq 2$ by taking $c = 1$, $m = 5$, while the other constants remain same.

Model 3: $\Gamma = 3\beta H\frac{\left(H^{2\lambda+2}-\frac{A}{3^{\lambda+1}}\right)^{\omega+1}-\frac{1}{3^{\mu}}}{\left(H_0^{2\lambda+2}-\frac{A}{3^{\lambda+1}}\right)^{\omega+1}-\frac{1}{3^{\mu}}}$

For this model, Equation (57) turns out to be:

$$\begin{aligned}\dot{S_T} &= -\frac{3y_0(r-\beta)}{2r^2}\left(\frac{y_0}{r}+\frac{1}{3^{\mu}}\right)^{\frac{-\omega}{1+\omega}}\left(\frac{A}{3^{1+\lambda}}+\left(\frac{y_0}{r}+\frac{1}{3^{\mu}}\right)^{\frac{\omega}{1+\omega}}\right)^{\frac{-\lambda}{1+\lambda}} \\ &\times\left(1+\frac{3^{\omega(1+\lambda)+1}}{T_0 r^{\frac{1-\mu}{\mu}}}\left(\frac{y_0}{r}+\frac{1}{3^{\mu}}\right)^{\frac{\omega-1}{1+\omega}}\left(\frac{y_0}{2r}\left(\frac{y_0}{r}+\frac{1}{3^{\mu}}\right)^{\frac{-\omega}{1+\omega}}\left(\frac{A}{3^{1+\lambda}}\right.\right.\right. \\ &\left.\left.\left.+\left(\frac{y_0}{r}+\frac{1}{3^{\mu}}\right)^{\frac{\omega}{1+\omega}}\right)^{-1}+1\right)\right).\end{aligned} \tag{60}$$

The plot of $\dot{S_T}$ versus a for three different values of λ is shown in Figure 12 for Model 3. The graph exhibits negative behavior, which does not show the validity in the given range by keeping the same constants.

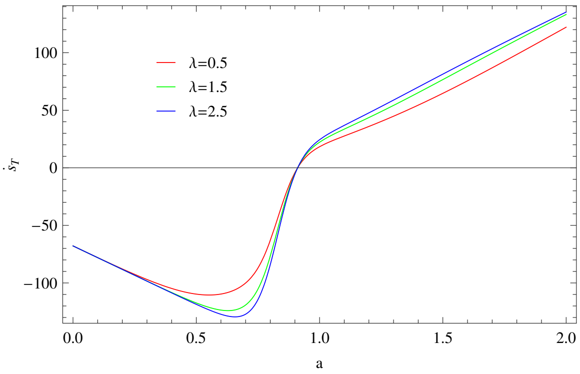

Figure 10. $\dot{S}$ versus a for Model 1.

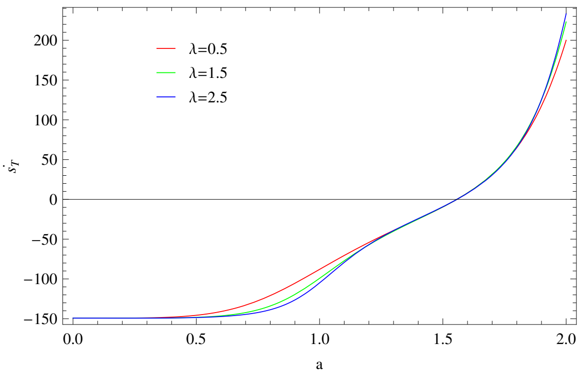

Figure 11. $\dot{S}$ versus a for Model 2.

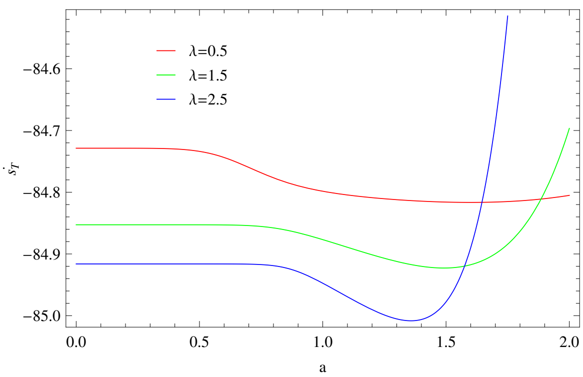

Figure 12. $\dot{S}$ versus a for Model 3.

4.1. Thermal Equilibrium

The thermal equilibrium scenario is discussed in this section. The thermodynamical equilibrium states that the entropy of the system attains the maximum value, and mathematically, it can be expressed as $\ddot{S_T} = \ddot{S_A} + \ddot{S_f} < 0$. Hence, the general expression can be written as:

$$\begin{aligned}\ddot{S_T} &= \frac{3}{4}\left(\frac{\dot{H}}{H^2}\right)^2 - \frac{\ddot{H}}{4H^3} + \frac{(3^{1+\lambda}H^{2+2\lambda}-A)^{\omega+1}-1}{3^{\lambda}H^{2+2\lambda}T_f(3^{1+\lambda}H^{2+2\lambda}-A)^{\omega}} \\ &\times\left(\frac{\dot{H}^2}{H^3} - \frac{\ddot{H}}{2H^2} + \frac{3}{2}\frac{d}{dt}\left(\frac{\Gamma}{3H}\right)\right) - \left(\frac{\dot{H}}{2H^2} + \frac{3}{2} - \frac{\Gamma}{2H}\right) \\ &\times\left(\frac{6\mu\dot{H}}{HT_f} - \frac{(3^{1+\lambda}H^{2+2\lambda}-A)^{\omega+1}-1}{3^{\lambda}H^{2+2\lambda}T_f^2(3^{1+\lambda}H^{2+2\lambda}-A)^{\omega}}\left(\dot{T_f} + 2\omega\right.\right. \\ &\left.\left.\times(1+\lambda)T_f\dot{H}\left(\frac{3^{1+\lambda}H^{2\lambda+1}}{3^{1+\lambda}H^{2+2\lambda}-A} + \frac{1}{\omega H}\right)\right)\right).\end{aligned} \tag{61}$$

Here, the terms used in the above expression are defined as:

$$\dot{H} = \left(1 - \frac{\Gamma}{3H}\right)\frac{(3^{\lambda+1}H^{2\lambda+2} - A)^{\omega+1} - 1}{2 * 3^{\lambda}H^{2\lambda}(3^{\lambda+1}H^{2\lambda+2} - A)^{\omega}}, \tag{62}$$

$$\begin{aligned}\ddot{H} &= \left(1 - \frac{\Gamma}{3H}\right)\left(3\mu H + ((3^{\lambda+1}H^{2\lambda+2} - A)^{\omega+1} - 1)\right. \\ &\left.\times\left(\frac{3\omega(1+\lambda)}{(3^{\lambda+1}H^{2\lambda+2}-A)^{\omega+1}} + \frac{3^{-\lambda}\lambda H^{1-2\lambda}}{(3^{\lambda+1}H^{2\lambda+2}-A)^{\omega}}\right)\right),\end{aligned} \tag{63}$$

$$\begin{aligned}\dot{T} &= 2T_c\dot{H}((3^{\lambda+1}H^{2\lambda+2} - A)^{\omega+1} - 1)^{1-\frac{1}{\mu}}\left(3H(\mu-1)\right. \\ &\times((3^{\lambda+1}H^{2\lambda+2} - A)^{\omega+1} - 1)^{-1} - (3^{\lambda+1}H^{2\lambda+2} - \tfrac{A}{2}) \\ &\left.\times 3^{-\lambda}H^{-2\lambda-1}(3^{\lambda+1}H^{2\lambda+2} - A)^{-\omega-1}\right).\end{aligned} \tag{64}$$

Here, H and T_f are taken from Equations (21) and (23).

4.1.1. Model 1: $\Gamma = 15\beta H\Big(1 - a\tanh(10 - 12a)\Big)$

We assume $\theta = 10 - 12a$, and using the following expression in Equation (61):

$$\frac{d}{dt}\left(\frac{\Gamma}{3H}\right) = -5\beta a H\left(\tanh\theta - \frac{12a}{\cosh\theta}\right) \tag{65}$$

Here, H and T_f are taken from Equations (26) and (28). The plot of $\ddot{S_T}$ versus a for three different values of λ is shown in Figure 13 for Model 1. The graph shows the validity of thermal equilibrium in the range of $0 \leq a \leq 0.7$ by taking the same constants as in Figure 1.

4.1.2. Model 2: $\Gamma = 3\beta H\Big(1 + a^{1+m}\Big)$

For this model, we have:

$$\frac{d}{dt}\left(\frac{\Gamma}{3H}\right) = \frac{\beta(m+1)a^{(m+1)}}{\sqrt{3}}H, \tag{66}$$

and H, T_f can be taken from Equations (31) and (33). By utilizing all the required values in (61), we get the expression of thermal equilibrium for this model. The plot of $\ddot{S_T}$ versus a for three different values of λ of Model 2 is shown in Figure 14. The graph shows the compatibility of thermal equilibrium in the range of $0 \leq a \leq 1.2$ by taking the same constants.

4.1.3. Model 3: $\Gamma = 3\beta H \frac{\left(H^{2\lambda+2} - \frac{A}{3^{\lambda+1}}\right)^{\omega+1} - \frac{1}{3^{\mu}}}{\left(H_0^{2\lambda+2} - \frac{A}{3^{\lambda+1}}\right)^{\omega+1} - \frac{1}{3^{\mu}}}$

Similarly, the expressions used in Equation (63) turn out to be:

$$\frac{d}{dt}\left(\frac{\Gamma}{3H}\right) = \left(1 - \frac{\Gamma}{3H}\right)\frac{\sqrt{3}\mu\beta}{y_0}H\left(3^{\lambda+1}H^{2\lambda+2} - A\right)^{\omega+1} - 1, \tag{67}$$

and here, H and T_f are taken from Equations (36) and (38). The plot of $\ddot{S_T}$ versus a for three different values of λ of Model 3 is shown in Figure 15, which shows the validity of the thermal equilibrium in the range of $0 \leq a \leq 2$.

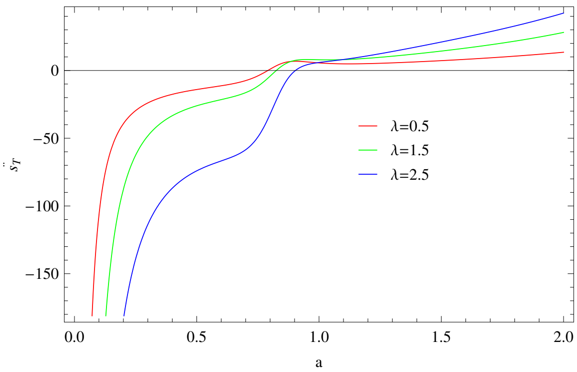

Figure 13. $\ddot{S}$ versus a for Model 1.

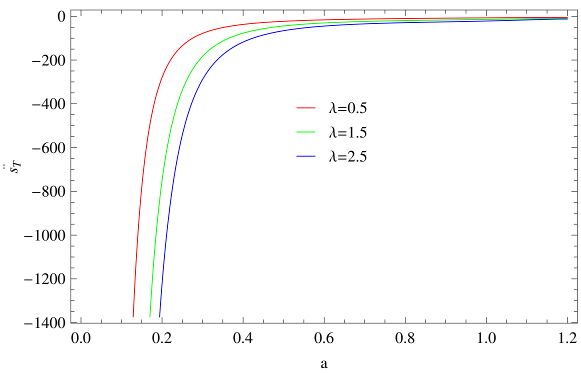

Figure 14. $\ddot{S}$ versus a for Model 2.

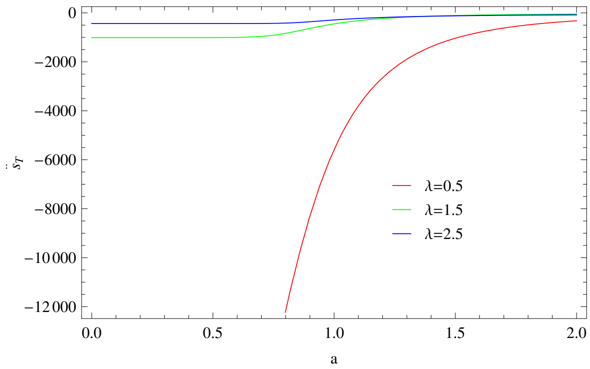

Figure 15. $\ddot{S}$ versus a for Model 3.

5. Summary

It was found that the particle creation mechanism has been extensively utilized in order to investigate the dynamics and evolution of the early universe including early inflation and the current accelerated expansion [55]. Recently, Bhattacharya et al. [58] studied the cosmic scenario and thermodynamics with adiabatic matter creation in the presence of MCG. Jawad et al. [59] discussed the thermodynamics of the gravitationally-induced particle creation scenario in the DGP braneworld. In the present work, we considered the cosmological implications of bulk viscous pressure due to the particle creation mechanism in a universe with matter described by GCCG. We discussed the dynamical and thermodynamical parameters by taking GCCG as a cosmic fluid under the particle creation mechanism. We developed declaration parameter (q), temperature (T_f), and particle number density (n) in the presence of three different models of the particle creation rate (Γ) and examined their behavior graphically. It was observed that the deceleration parameter exhibited the accelerated expansion behavior of universe with the passage of time for Models 1 and 2 (Figures 1 and 4), while decelerating behavior of the universe for Model 3 of Γ (Figure 7). The observational constraints on the deceleration parameter have been mentioned in the literature [73]. The ranges of the decelerating parameter (for Models 1 and 2) lied within the constraints as mentioned in [73]. However, the temperature and particle number density remained positive in all cases of Γ. We examined the validity of GSLT with respect to the scale factor by assuming Bekenstein entropy as the horizon entropy. It was found that GSLT remained valid for Model 1 (Figure 10) in the range $0.91 \leq a \leq 2$, and Model 2 exhibited validity in the range of $1.4 \leq a \leq 2$ (Figure 11), while Model 3 did not show the validity of GSLT (Figure 12). The stability of thermal equilibrium was also examined for the three model of the particle creation rate. It was found that Model 1 showed the validity in the range of $0 \leq a \leq 0.7$ (Figure 13), while Models 2 and 3 led to the validity in the whole range of the scale factor.

Author Contributions: A.J. and S.R. have completed the manuscript; M.A.S. helped in the calculations of manuscript.

Funding: This research was funded by HEC Islamabad, Pakistan for its financial support under the grant No.5412/federal/nrpu/R&D/HEC/2016.

Conflicts of Interest: The authors declare no conflict of interest.

References

1. Muller, I.; Physik, Z. Zum Paradoxon der Warmeleitungstheorie. *Z. Phys.* **1967**, *198*, 329–344. [CrossRef]
2. Israel, W. Nonstationary irreversible thermodynamics: A Causal relativistic theory. *Ann. Phys.* **1976**, *100*, 310–331. [CrossRef]
3. Israel, W.; Stewart, J.M. Transient relativistic thermodynamics and kinetic theory. *Ann. Phys.* **1979**, *118*, 341–372. [CrossRef]

4. Hiscock, W.A.; Lindblom, L. Stability and causality in dissipative relativistic fluids. *Ann. Phys.* **1983**, *151*, 446–496. [CrossRef]
5. Pavon, D.; Jou, D.; Casas-Vazquesz, J. On a covariant formulation of dissipative phenomena. *Ann. Inst. H Poineer Sec. A* **1982**, *36*, 79–88.
6. Pavon, D.; Bafaluy, J.; Jou, D. Causal Friedmann-Robertson-Walker cosmology. *Astron. J.* **1991**, *8*, 347. [CrossRef]
7. Riess, A.G.; Filippenko, A.V.; Challis, P.; Clocchiatti, A.; Diercks, A.; Garnavich, P.M.; Gilliland, R.L.; Hogan, C.J.; Jha, S.; Kirshner, R.P.; et al. Observational Evidence from Supernovae for an Accelerating Universe and a Cosmological Constant. *Astron. J.* **1998**, *116*, 1009. [CrossRef]
8. Perlmutter, S.; Aldering, G.; Goldhaber, G.; Knop, R.A.; Nugent, P.; Castro, P.G.; Deustua, S.; Fabbro, S.; Goobar, A.; Groom, D.E.; et al. Measurements of Ω and Λ from 42 High-Redshift Supernovae. *Astrophys. J.* **1999**, *517*, 565. [CrossRef]
9. Spergel, D.N.; Verde, L.; Peiris, H.V.; Komatsu, E.; Nolta, M.R.; Bennett, C.L.; Halpern, M.; Hinshaw, G.; Jarosik, N.; Kogut, A.; et al. First-Year Wilkinson Microwave Anisotropy Probe (WMAP) Observations: Determination of Cosmological Parameters. *Astrophys. J. Suppl.* **2003**, *148*, 175. [CrossRef]
10. Adelman-McCarthy, J.K.; Agüeros, M.A.; Allam, S.S.; Prieto, C.A.; Anderson, K.S.; Anderson, S.F. Annis, J.; Bahcall, N.A.; Bailer-Jones, C.A.L.; Baldry, I.K.; et al. The Sixth Data Release of the Sloan Digital Sky Survey. *Astrophys. J. Suppl.* **2008**, *175*, 297. [CrossRef]
11. Sahni, V.; Starobinsky, A.A. The Case for a Positive Cosmological Lambda-term. *Int. J. Mod. Phys. A* **2000**, *9*, 373. [CrossRef]
12. Peebles, P.J.E.; Ratra, B. 100 years of Gravity and Accelerated Frames, The deepest insights of Einstein and Yang-Mills. *Rev. Mod. Phys.* **2003**, *75*, 559. [CrossRef]
13. Padmanabhan, T. Cosmological constant-the weight of the vacuum. *Phys. Rept.* **2003**, *380*, 235–320. [CrossRef]
14. Copeland, E.J.; Sami, M.; Tsujikawa, S. Dynamics of dark energy. *Int. J. Mod. Phys. D* **2006**, *15*, 1753–1935. [CrossRef]
15. Elizalde, E.; Nojiri, S.; Odinstov, S.D. Late-time cosmology in a (phantom) scalar-tensor theory: Dark energy and the cosmic speed-up. *Phys. Rev. D* **2004**, *70*, 043539. [CrossRef]
16. Nojiri, S.; Odintsov, S.D.; Tsujikawa, S. Properties of singularities in (phantom) dark energy universe. *Phys. Rev. D* **2005**, *71*, 063004. [CrossRef]
17. Anisimov, A.; Babichev, E.; Vikman, A. B-inflation. *J. Cosmol. Astropart. Phys.* **2005**, *06*, 006. [CrossRef]
18. Zlatev, I.; Wang, L.; Steinhardt, P.J. Quintessence, Cosmic Coincidence, and the Cosmological Constant. *Phys. Rev. Lett.* **1999**, *82*, 896. [CrossRef]
19. Turner, M.S. Making Sense of The New Cosmology. *Int. J. Mod. Phys. A* **2002**, *17*, 180–196. [CrossRef]
20. Sahni, V. The Cosmological Constant Problem and Quintessence. *Class. Quant. Grav.* **2002**, *19*, 3435. [CrossRef]
21. Setare, M.R. Interacting generalized Chaplygin gas model in non-flat universe. *Eur. Phys. J. C* **2007**, *52*, 689–692. [CrossRef]
22. Bernardini, A.E.; Bertolami, O. Perturbative approach for mass varying neutrinos coupled to the dark sector in the generalized Chaplygin gas scenario. *Phys. Rev. D* **2008**, *77*, 083506. [CrossRef]
23. Bernardini, A.E. Dynamical neutrino masses in the generalized Chaplygin gas scenario with mass varying CDM. *Astropart. Phys.* **2011**, *34*, 431–437. [CrossRef]
24. Armendariz-Picon, C.; Damour, T.; Mukhanov, V. k-Inflation. *Phys. Lett. B* **1999**, *458*, 209. [CrossRef]
25. Armendariz-Picon, C.; Mukhanov, V.; Steinhardt, P.J. Dynamical Solution to the Problem of a Small Cosmological Constant and Late-Time Cosmic Acceleration. *Phys. Rev. Lett.* **2000**, *85*, 4438. [CrossRef]
26. Chiba, T.; Okabe, T.; Yamaguchi, M. Kinetically driven quintessence. *Phys. Rev. D* **2000**, *62*, 023511. [CrossRef]
27. Hsu, S.D.H. Entropy Bounds and Dark Energy. *Phys. Lett. B* **2004**, *594*, 13. [CrossRef]
28. Li, M. A Model of Holographic Dark Energy. *Phys. Lett. B* **2004**, *603*, 1. [CrossRef]
29. Horndeski, G.W. Second-order scalar-tensor field equations in a four-dimensional space. *Int. J. Theor. Phys.* **1974**, *10*, 363–384. [CrossRef]
30. Nojiri, S.; Odintsov, S.D. Unified cosmic history in modified gravity: from F(R) theory to Lorentz non-invariant models. *Phys. Rept.* **2011**, *505*, 59–144. [CrossRef]
31. Sebastiani, L.; Vagnozzi, S.; Myrzakulov, R. Mimetic Gravity: A Review of Recent Developments and Applications to Cosmology and Astrophysics. *Adv. High Energy Phys.* **2017**, *2017*, 3156915. [CrossRef]

32. Cai, Y.F.; Capozziello, S.; De Laurentis, M.; Saridakis, E.N. f(T) teleparallel gravity and cosmology. *Rept. Prog. Phys.* **2016**, *79*, 106901. [CrossRef]
33. Nojiri, S.; Odintsov, S.D. Gauss-Bonnet dark energy. *Phys. Rev. D* **2005**, *71*, 123509. [CrossRef]
34. Bamba, K.; Capozziello, S.; Nojiri, S.I.; Odintsov, S.D. Dark energy cosmology: the equivalent description via different theoretical models and cosmography tests. *Astrophy. Space Sci.* **2012**, *342*, 155–228. [CrossRef]
35. Debnath, U.; Banerjee, A.; Chakraborty, S. Chakraborty, S. Role of Modified Chaplygin Gas in Accelerated Universe. *Class. Quantum Grav.* **2004**, *21*, 5609. [CrossRef]
36. Bento, M.C.; Bertolami, O.; Sen, A.A. Generalized Chaplygin gas, accelerated expansion, and dark-energy-matter unification. *Phys. Rev. D* **2002**, *66*, 043507. [CrossRef]
37. Sen, A.A.; Scherrer, R.J. Generalizing the generalized Chaplygin gas. *Phys. Rev. D* **2005**, *72*, 063511. [CrossRef]
38. Benaoum, H.B. Modified Chaplygin Gas Cosmology with Bulk Viscosity. *Int. J. Mod. Phys. D* **2014**, *23*, 1450082. [CrossRef]
39. Lu, J.; Xu, L.; Wu, Y.; Liu, M. Constraints on modified Chaplygin gas from recent observations and a comparison of its status with other models. *Phys. Lett. B* **2008**, *662*, 87–91. [CrossRef]
40. Kamenshchik, A.Y.; Moschella, U.; Pasquier, V. An alternative to quintessence. *Phys. Lett. B* **2001**, *511*, 265–268. [CrossRef]
41. Bertolami, O.; Duvvuri, V. Chaplygin inspired Inflation. *Phys. Lett. B* **2006**, *640*, 121–125. [CrossRef]
42. Gonzalez-Diaz, P.F. You need not be afraid of phantom energy. *Phys. Rev. D* **2003**, *68*, 021303. [CrossRef]
43. Hawking, S.W. Particle creation by black holes. *Commun. Math. Phys.* **1975**, *43*, 199–220. [CrossRef]
44. Jacobson, T. Thermodynamics of Spacetime: The Einstein Equation of State. *Phys. Rev. Lett.* **1995**, *75*, 1260. [CrossRef]
45. Padmanabhan, T. Classical and Quantum Thermodynamics of horizons in spherically symmetric spacetimes. *Class. Quantum Grav.* **2002**, *19*, 5387. [CrossRef]
46. Bekenstein, J.D. Black Holes and Entropy. *Phys. Rev. D* **1973**, *7*, 2333. [CrossRef]
47. Cai, R.G.; Kim, S.P. First Law of Thermodynamics and Friedmann Equations of Friedmann-Robertson-Walker Universe. *JHEP* **2005**, *02*, 050. [CrossRef]
48. Banerjee, R.; Modak, S.K. Quantum Tunneling, Blackbody Spectrum and Non-Logarithmic Entropy Correction for Lovelock Black Holes. *JHEP* **2009**, *073*, 0911. [CrossRef]
49. Sheykhi, A.; Jamil, M. Power-Law entropy corrected holographic dark energy model. *Gen. Relativ. Gravit.* **2011**, *43*, 2661. [CrossRef]
50. Karami, K.; Ghaffari, S.; Soltanzadeh, M.M. The generalized second law of gravitational thermodynamics on the apparent and event horizons in FRW cosmology. *Class. Quantum Grav.* **2010**, 27, 205021. [CrossRef]
51. Jamil, M.; Saridakis, E.N.; Setare, M.R. Thermodynamics of dark energy interacting with dark matter and radiation. *Phys. Rev. D* **2010**, *81*, 023007. [CrossRef]
52. Zeldovich, Y.A. The Neutrino Mass in Elementry particle physics and in Bing Bang Cosmology. *Sov. Astron. Lett.* **1981**, *7*, 332.
53. Prigogine, I.; Geheniau, J.; Gunzig, E.; Nardone, P. Thermodynamics and cosmology. *Gen. Relativ. Gravit.* **1989**, *21*, 767 [CrossRef]
54. Lima, J.A.S.; Jesus, J.F.; Oliveira, F.A. CDM accelerating cosmology as an alternative to ΛCDM model. *J. Cosmol. Astropart. Phys.* **2010**, *11*, 027. [CrossRef]
55. Chakraborty, S.; Saha, S. Complete cosmic scenario from inflation to late time acceleration: Nonequilibrium thermodynamics in the context of particle creation. *Phys. Rev. D* **2014**, *90*, 123505. [CrossRef]
56. Chakraborty, S. Is emergent universe a consequence of particle creation process? *Phys. Lett. B* **2014**, *732*, 81–84. [CrossRef]
57. Brevik, I. Cosmology for Early- and Late-Time Universe. *Int. J. Mod. Phys. D* **2017**, *26*, 1730024. [CrossRef]
58. Bhattacharya, S.; Halder, S.; Chakraborty, S. Evolving cosmic scenario in modified Chaplygin gas with adiabatic matter creation. *Ann. Phys.* **2018**, *388*, 443–455. [CrossRef]
59. Jawad, A.; Rani, S.; Rafique, S. Thermodynamics of Various Entropies in Specific Modified Gravity with Particle Creation. *Eur. Phys. J. C* **2018**, *78*, 79. [CrossRef]
60. Steigman, G.; Santos, R.C.; Lima, J.A.S. An Accelerating Cosmology Without Dark Energy. *J. Cosmol. Astropart. Phys.* **2009**, *06*, 033. [CrossRef]
61. Lima, J.A.S.; Graef, L.L.; Pavon, D.; Basilakos, S. Cosmic acceleration without dark energy: Background tests and thermodynamic analysis. *J. Cosmol. Astropart. Phys.* **2014**, *10*, 042. [CrossRef]

62. Chakraborty, S.; Pan, S.; Saha, S. A third alternative to explain recent observations: Future deceleration. *Phys. Lett. B* **2014**, *738*, 424–427. [CrossRef]
63. Nunes, R.C.; Pavon, D. Phantom behavior via cosmological creation of particles. *Phys. Rev. D* **2015**, *91*, 063526. [CrossRef]
64. Lima, J.A.S.; Basilakos, S. Constraints on cold dark matter accelerating cosmologies and cluster formation. *Phys. Rev. D* **2010**, *82*, 023504.
65. Lima, J.A.S.; Basilakos, S.; Costa, F.E.M. New cosmic accelerating scenario without dark energy. *Phys. Rev. D* **2012**, *86*, 103534. [CrossRef]
66. Jesus, J.F.; Oliveira, F.A.; Basilakos, S.; Lima, J.A.S. Newtonian perturbations on models with matter creation. *Phys. Rev. D* **2011**, *84*, 063511. [CrossRef]
67. Nunes, R.C.; Pan, S. Cosmological consequences of an adiabatic matter creation process. *Mon. Not. R. Asron. Soc.* **2016**, *459*, 673–682. [CrossRef]
68. Nunes, R.C. Connecting inflation with late cosmic acceleration by particle production. *Int. J. Mod. Phys. D* **2016**, *25*, 1650067. [CrossRef]
69. Fabris, J.C.; Pacheco, J.A.F.; Piattella, O.F. Is the continuous matter creation cosmology an alternative to ΛCDM? *J. Cosmol. Astropart. Phys.* **2014**, *06*, 038. [CrossRef]
70. Abramo, L.R.W.; Lima, J.A.S. Inflationary Models Driven by Adiabatic Matter Creation. *Class. Quant. Grav.* **1996**, *13*, 2953. [CrossRef]
71. Mimoso, J.P.; Pavon, D. Entropy evolution of universes with initial and final de Sitter eras. *Phys. Rev. D* **2013**, *87*, 047302. [CrossRef]
72. Gunzig, E.; Maartens, R.; Nesteruk, A.V. Inflationary cosmology and thermodynamics. *Class. Quant. Grav.* **1998**, *15*, 923. [CrossRef]
73. Aviles, A.; Gruber, O.; Luongo, H.Q. Cosmography and constraints on the equation of state of the Universe in various parametrizations. *Phys. Rev. D* **2012**, *86*, 123516. [CrossRef]
74. Modak, S.K.; Singleton, D. Inflation with a graceful exit and entrance driven by Hawking radiation. *Phys. Rev. D* **2012**, *86*, 123515.